Accepted Preprint first posted on 7 November 2013 as Manuscript JOE-13-0400

MCT 8 in human fetal cerebral cortex is reduced in severe intrauterine growth restriction

Shiao Y. Chan[1], Laura A. Hancox[1], Azucena Martín-Santos[1], Laurence S. Loubière[1], Merlin N.M. Walter[1], Ana-Maria González[1], Phillip M. Cox[2], Ann Logan[1], Christopher J. McCabe[1], Jayne A. Franklyn[1], Mark D. Kilby[1,3]

[1]School of Clinical and Experimental Medicine, College of Medical and Dental Sciences, University of Birmingham, Edgbaston, Birmingham, B15 2TT, UK

[2]Department of Pathology, Birmingham Women's NHS Foundation Trust, Edgbaston, Birmingham, B15 2TG, UK.

[3]Fetal Medicine Centre, Birmingham Women's NHS Foundation Trust, Edgbaston, Birmingham, B15 2TG, UK.

Abbreviated Title: MCT8 in IUGR human fetal brain

Key words: MCT8, human fetus, central nervous system, intrauterine growth restriction (IUGR)

Word count: 3555

Correspondence and reprint requests to: Dr Shiao Chan

Address: School of Clinical and Experimental Medicine, University of Birmingham, Floor 3, Birmingham Women's Foundation Trust, Metchley Park Road, Edgbaston, Birmingham B15 2TG, United Kingdom.

Tel No: (+44)-121-4158631 Facsimile No: (+44)-121-4158712 E-mail: s.chan@bham.ac.uk

ABSTRACT

The importance of the thyroid hormone (TH) transporter, monocarboxylate transporter (MCT8), to human neurodevelopment is highlighted by findings of severe global neurological impairment in subjects with MCT8 mutations. Intrauterine growth restriction (IUGR), usually due to uteroplacental failure, is associated with milder neurodevelopmental deficits, which have been partly attributed to dysregulated TH action *in utero* secondary to reduced circulating fetal TH concentrations and decreased cerebral TH receptor expression. We postulate that altered MCT8 expression is implicated in this pathophysiology and sought to quantify changes in cortical MCT8 expression with IUGR.

Firstly, MCT8 immunohistochemistry was performed on occipital and parietal cerebral cortex sections from appropriately grown for gestational age (AGA) human fetuses between 19 weeks gestation and term. Secondly, MCT8 immunostaining in the occipital cortex of stillborn IUGR human fetuses at 24-28 weeks gestation were objectively compared with gestationally-matched AGA fetuses.

Fetuses demonstrated widespread MCT8 expression in neurons within the cortical plate and subplate, in the ventricular and subventricular zones, epithelium of the choroid plexus and ependyma, and microvessel wall. When complicated by IUGR, fetuses showed a significant 5-fold reduction in the percentage area of cortical plate immunostained with MCT8 compared with AGA fetuses ($p<0.05$) but there was no significant difference in the proportion of subplate microvessels immunostained. Cortical MCT8 expression negatively correlated with the severity of IUGR indicated by brain:liver weight ratios ($r^2=0.28$, $p<0.05$) at post-mortem. Our results support the hypothesis that a reduction in MCT8 expression in the IUGR fetal brain could further compromise TH-dependent brain development.

INTRODUCTION

Intrauterine growth restriction (IUGR) describes the failure of a fetus to attain its genetically-determined growth potential; the most common underlying aetiology being uteroplacental failure associated with abnormal placental development. IUGR is often characterized by continued head and brain growth at the expense of other less vital organs resulting in an elevated brain:liver weight ratio postnatally (Cox & Marton 2009). IUGR complicates 5-10% of pregnancies and is associated with increased perinatal mortality (Kady & Gardosi 2004). Survivors demonstrate an increased prevalence of cognitive impairment compared with babies born appropriately grown for gestational age (AGA). They have lower school achievements and IQ scores (Leitner *et al.* 2007), and 5% show neurodevelopmental delay at age 9-10 years (Kok *et al.* 1998). Significantly reduced circulating concentrations of free T_4 and T_3 (Kilby *et al.* 1998) and decreased cerebral thyroid hormone receptor (TR) expression (Kilby *et al.* 2000) in growth-restricted human fetuses are postulated to contribute to this neurodevelopmental morbidity. Examination of growth-restricted fetal guinea pigs showed a compensatory increase in brain deiodinase type 2 (D2) expression, which could increase local concentrations of the active thyroid hormone (TH) ligand, T_3, from T_4 conversion (Chan *et al.* 2005). In clinical practice, once IUGR is diagnosed antenatally, timely delivery aimed at avoiding *in utero* demise whilst prolonging gestation as far as possible for fetal maturity, is the mainstay of management. Currently, there are no *in utero* therapies to reduce the risk of neurocognitive impairment in IUGR. An increased understanding of how TH-responsive neurodevelopment is altered in IUGR may lead to the development of novel therapies to improve long-term outcome.

Monocarboxylate transporter 8 (MCT8) is a highly specific plasma membrane TH transporter (Friesema *et al.* 2003). Its importance to human central nervous system (CNS) development has been highlighted by discoveries of different mutations within the MCT8 gene (SLC16A2) in subjects with a variety of X-linked mental retardation syndromes, characterized by severe psychomotor and cognitive impairment and

accompanied by elevated serum free T_3 but normal or low free T_4 concentrations (Dumitrescu *et al.* 2004; Friesema *et al.* 2004; Schwartz *et al.* 2005).

In mice, mct8 facilitates TH entry into the brain parenchyma across the blood brain barrier (Ceballos *et al.* 2009), and at a cellular level, TH entry into neurons (Trajkovic *et al.* 2007), where mct8 is responsible for 75% of T_3 uptake (Wirth *et al.* 2009). In rodents, TH affects cell proliferation and differentiation of neuroblastoma cells (Garcia-Silva *et al.* 2002) and oligodendrocytes (Jones *et al.* 2003), neuronal migration (Auso *et al.* 2004; Lavado-Autric *et al.* 2003), synaptogenesis (Gilbert & Paczkowski 2003) and cerebellar Purkinje cell dendritic outgrowth (Heuer & Mason 2003). T_3 has a pro-proliferative effect in human neuronal precursor cells, NT2, but MCT8, independently of T_3, could repress NT2 proliferation (James *et al.* 2009), suggesting another role for MCT8 apart from TH transport. However, the lack of neurological defects in mct8 knock-out mice (Wirth *et al.* 2009) emphasizes the need for studies in humans. From 7 weeks gestation the human fetal cerebral cortex is potentially TH-responsive, expressing a range of TH transporters including MCT8 (Chan *et al.* 2011), all the major TR isoforms (nuclear transcription factors that bind T_3 to regulate gene transcription) and demonstrate pre-receptor regulation by D2 and deiodinase type 3 (D3; which inactivates T4 and T3) (Chan *et al.* 2002). Fetal neurons are believed to be the main target for TH action in the brain.

We hypothesize that human fetal cortical MCT8 expression is reduced with severe IUGR, which could further compromise neurodevelopment. In this study, we first localized MCT8 expression in the human fetal cerebral cortex from mid-gestation onwards. We then compared cortical MCT8 expression in severe IUGR with that in AGA human fetuses who were stillborn.

MATERIALS AND METHODS

Brain samples

This study was approved by the South Birmingham Research Ethics Committee. Written consent for blocks and slides to be used in research and teaching was obtained in all cases. Cases were identified

retrospectively from reports of all post-mortems conducted at the Birmingham Women's Hospital over a three year period. Only a minority of cases fulfilled our strict inclusion criteria: normal karyotype, no histopathological evidence of intrauterine infection and limited or no maceration (indicating very short death to delivery intervals). Gestational ages were determined by 1st trimester ultrasound scan for crown-rump length. Sections of formalin-fixed paraffin-embedded (FFPE) samples were then obtained from the hospital archive of histopathology blocks.

Firstly, sections of the fetal cerebral cortex (occipital and parietal) from the second (19-20 weeks; n=3) and third trimesters (26-37 weeks; n=3) from AGA fetuses with unexplained intrauterine deaths were examined. Sections of normal adult occipital cortex (one female aged 55 years and one male aged 37 years) sampled at post-mortem and donated to the London Neurodegenerative Diseases Brain Bank (Institute of Psychiatry, King's College London) were obtained for comparison.

Secondly, sections of the occipital cerebral cortex from stillborn human fetuses between 24-28 weeks gestation were obtained and categorized as either IUGR (n=7) or AGA (n=5) (Table 1). IUGR was defined as having: (i) a birth weight below the third percentile for gestation, based on customized growth charts, which account for maternal weight, height, parity, ethnicity, gestation and fetal sex (Gardosi *et al.* 1992), (ii) a brain:liver weight ratio greater than four (Cox & Marton 2009). Although we have not prospectively documented the presence of fetal growth restriction prenatally prior to death, the post-mortem features are highly suggestive of this pathology. IUGR is likely to be significant as the phenotype was associated with fetal demise.

Immunohistochemistry

FFPE sections (5µm) of cortical samples were immunostained for MCT8 using an avidin-biotin peroxidase technique (Vectastain Elite; all reagents from Vector Laboratories, Peterborough, UK unless otherwise stated) as per the kit instructions as previously described (Chan *et al.* 2011). Briefly, after dewaxing and serial rehydration, sections were incubated in 10mM sodium citrate buffer (pH 6.0) in a

95ºC water bath for10 minutes. After washing in 50mM Tris/0.15M saline (pH 7.5; TBS), the sections were blocked with 10% normal goat serum (Sigma-Aldrich, UK) in diluting buffer (TBS, 0.3%Tween 20, 2%BSA) for 20 minutes. Then consecutive sections were incubated overnight at 4ºC with rabbit anti-MCT8 (4790) (Sigma-Genosys Ltd., Haverhill, UK) (Chan *et al.* 2011; Vasilopoulou *et al.* 2010) at 1μg/ml, anti-glial fibrillary acidic protein (GFAP, glia marker; Dako M0761 at 1:120) or anti-CD68 (microglia marker; Dako M0876 at 1:100). Sections were incubated with biotinylated goat anti-rabbit secondary antibody at 1:200 for 30 minutes followed by 5% hydrogen peroxide for 5 minutes then the avidin-biotin-peroxidase complex for 30 minutes. Immunoreactivity was visualized with 3,3'-diaminobenzidine (15 minutes). All steps were separated by TBS-Tween washes. Sections for localization studies were lightly counterstained with Mayer's Hematoxylin and mounted in Vectamount. Slides for comparisons of IUGR with AGA were mounted with aqueous Vectashield H1000 without counterstaining. Sections were examined under bright field microscopy using a Zeiss microscope and images captured using AxioVision software. The specificity of this MCT8 antiserum (4790) has been determined previously (Chan *et al.* 2011; Vasilopoulou *et al.* 2010) and confirmed in these studies by pre-incubating the primary antibody with blocking peptide (25μg/ml) before application to adjacent sections. Negative controls for each tissue sample were also performed by omitting the primary antibody.

Quantifying MCT8 immunostaining

Comparisons of IUGR with AGA focused on the occipital cerebral cortex, which is involved in visual perception and interpretation. The *in utero* development of this structure is thought to be TH-responsive (Zoeller & Rovet 2004) and affected in IUGR (Dowdeswell *et al.* 1995). We quantified: (i) the percentage area stained for MCT8 in the cortical plate, (ii) the proportion of microvessels stained for MCT8 in the subplate, with the researcher blinded to the experimental grouping.

MCT8 staining in the cortical plate

For each fetus, five images (20X magnification) from the MCT8 immunostained section and five corresponding images from the adjacent section processed with the omission of the primary antibody as a

negative control were analyzed. An objective measure of the area containing brown pixels corresponding to immunoreactive staining for MCT8, was quantified using the software ImageJ (U. S. National Institutes of Health, Bethesda, Maryland, USA), as previously described (National Institute of Health 2012). Briefly, bright field images were converted to grayscale 'RGB stack', and the green channel image used for analysis. A grayscale cut-off point derived from corresponding negative controls was set as the threshold signifying positive staining and the same threshold applied to the immunostained sections for each fetus. The total area of tissue stained above the threshold was quantified and expressed as a proportion of the total tissue area examined. The area fraction of background noise, as determined by applying the same threshold to the corresponding negative control, was subtracted from the area fraction of tissue stained to give the true proportion of area of tissue staining positively for MCT8. Since the area of staining could also be affected by cell density, the number of cell bodies (nuclei) within a 250 x 250 pixel field in each quadrant of every image analyzed was counted and averaged to determine the relative cellularity, which was used to correct the area stained with MCT8. The corrected percentage of area stained for each fetus was then expressed relative to the mean of the AGA group, which has been assigned an arbitrary value of 1.

MCT8 staining in microvessels

MCT8 immunoreactivity in microvessels was assessed in the subplate zone, a layer deep to the cortical plate with a lower density of cells, where it was easily possible to identify all the microvessels in bright field based on morphology at 40X magnification. Twenty non-overlapping images of the subplate were taken of each fetus. The number of immunostained microvessels were counted and calculated as a percentage of all microvessels present. An average of 40.4 ± 1.9 microvessels was counted per fetus. Non-specific staining of intravascular erythrocytes was disregarded. The percentage of microvessels stained was then expressed relative to the mean of the AGA group, which has been assigned an arbitrary value of 1.

Statistical Analyses

Data were analyzed using the Sigma Stat software v3.1. Demographic data were analyzed using the unpaired student t-test to compare continuous variables and the Fisher Exact test to compare contingency tables. Quantitative data expressed as relative values were used for analysis using the two-way ANOVA followed by Holm-Sidak all pairwise multiple comparisons post-hoc analysis. The quantitative data sets passed the normality and equal variance tests. Spearman rank correlation test was used to determine significant correlations between variables. Significance was taken as $p<0.05$.

RESULTS

MCT8 immunolocalization within human fetal and adult cerebral cortex

The developing human fetal cerebral cortex in mid-gestation is formed by several layers, from superficial to deep they are the marginal zone, cortical plate, subplate, intermediate zone, subventricular zone and ventricular zone (lying adjacent to the ventricle) (Bystron *et al.* 2008). At 19 weeks gestation, sections of the parietal and occipital cortex from AGA fetuses demonstrated MCT8 immunostaining in all layers. Immunostaining was found within the marginal zone, in cortical plate neurons, a proportion of cells in the subplate zone, in hippocampal neurons, epithelial cells of the choroid plexus and ependyma, and in numerous cells in the ventricular and subventricular zones (Figure 1A-D, H). A similar distribution of MCT8 immunostaining was observed from 26 to 37 weeks gestation in AGA fetuses. However, with advancing gestation and maturity of the cortex there were fewer cells in the ventricular and subventricular zones and, hence, correspondingly less MCT8 staining in these layers (Figure 1D-F). Most microvessels throughout the areas studied were MCT8 positive (Figure 1G). Absorption of the antibody with the blocking peptide effectively abolished MCT8 staining, confirming the specificity of staining (Figure 1A-C).

MCT8 immunostaining corresponded with the well-described pattern of neuronal cell distribution within the cerebral cortex, with the greatest staining in the cortical plate which is dense with neurons. A neuronal localization of MCT8 was also supported by our findings that immunostaining for GFAP and CD68, indicating glia and microglia respectively, in adjacent sections revealed an entirely different pattern of distribution in all layers of the cortex (Figure 1J-K) compared with MCT8 immunostaining. Specifically there was no GFAP or CD68 immunostaining in the cortical plate. In addition, the morphology of cells stained with each antibody was clearly different. Neurons were identified by a round dense nucleus, abundant cytoplasm with dendritic branching, many of which were immunostained with MCT8, in contrast to astrocytes which had a large irregular nucleus with clear nucleoplasm containing vesicular chromatin pattern and very small or absent nucleoli showing no MCT8 immunostaining (Figure 1H-I). At every gestation within the subplate only a selected population of neurons were MCT8 positive. In the adult occipital cortex, microvessels were immunostained but proportionally fewer neurons immunostained with MCT8 compared with the fetal cortex (data not shown).

Comparing MCT8 immunostaining in the occipital cortex of AGA and IUGR fetuses

There were no significant differences between the IUGR and AGA cohorts in terms of gestational age and fetal sex (Table 1). Compared with the AGA group, the IUGR group had significantly lower raw birthweights ($p<0.05$) (with customized birthweight percentiles all under the 3rd percentile) but the raw brain weights were not significantly different between the two groups with brain weights being well preserved for gestation even in the IUGR cohort (1.08 relative to expected mean). However, the relative brain weights (ratio to the expected mean for gestation) were still lower in the IUGR group compared with the AGA group ($p<0.05$). The brain:liver weight ratios were significantly higher in the IUGR group compared with the AGA group ($p<0.01$). Atrophy of the thymus secondary to chronic stress in IUGR (Cox & Marton 2009) was also evident by the significantly reduced raw thymus weights ($p<0.01$) and thymus weights relative to the expected mean for gestation ($p<0.001$). All of this indicates that the IUGR

cohort comprised cases at the severe end of the spectrum. Most of the IUGR cases demonstrated features of chronic uteroplacental failure on placental examination (Table 1 ReCoDe C4 and C5), which were absent in the AGA cohort.

The overall two-way ANOVA which analyzed the entire data set, indicated significantly reduced MCT8 expression in the occipital cortex of IUGR fetuses compared with AGA fetuses ($p<0.05$). However, post-hoc testing showed that the difference was significant for cortical plate immunostaining only ($p<0.05$; Figure 2).

The mean percentage area of cortical plate immunostaining after correction for relative cell number was 4.7±1.5% (mean±s.e.m.; 0.2±0.07 relative to AGA) in the IUGR group compared with 23.3±8.1% (1±0.3 relative to AGA) in the AGA group ($p<0.05$), which represents approximately a five-fold decrease in MCT8 expression with IUGR (Figure 2). The cellularity within the cortical plate was not significantly different between the two cohorts (IUGR: 1.3±0.1; AGA: 1±0.1). General observations of cortical plate images suggest that the decrease in MCT8 staining was confined to morphologically-defined neuronal cells, whilst microvessels seemed to be spared (Figure 3).

Post-hoc tests revealed no statistically significant difference in the proportion of microvessels stained for MCT8 in the IUGR samples (27.9±10.0%; 0.6±0.2 relative to AGA) compared with AGA samples (45.2±9.6%; 1±0.2 relative to AGA; Figure 2).

However, there was a significant positive correlation between the area of cortical plate MCT8 immunostaining and the proportion of microvessels stained in the subplate (correlation coefficient=0.71, $r^2=0.27$; $p<0.01$) when all samples were analyzed together. The positive correlation remained significant within the IUGR group (correlation coefficient=0.75, $r^2=0.12$; $p<0.05$; Figure 4A) but there was no significant correlation within the AGA cohort on its own.

When all samples were analyzed together, a negative correlation was also observed between the area of cortical plate MCT8 immunostaining and brain:liver weight ratios (correlation coefficient=-0.64, $r^2=0.28$;

$p<0.05$; Figure 4B). There was no correlation between MCT8 immunostaining in the cortical plate or microvessels with either gestational age or fetal sex.

DISCUSSION

Changes in TH transporter expression have never been described in the growth-restricted state. This study is the first to demonstrate significantly reduced cortical expression of MCT8 within the developing CNS of human fetuses stillborn with severe IUGR. Our results suggest altered TH transporter activity in cerebral neurons could be a contributory factor to the pathophysiology of neurodevelopmental impairment associated with IUGR.

The strength of this study is the use of human fetal tissue, thus eliminating species differences, particularly relevant as mct8 knockout mice lack the neurological phenotype seen in humans with MCT8 mutations. A limitation is, however, restriction of the availability of human fetal tissue of adequate quality for investigation, hence, the small numbers in this study.

MCT8 localization in developing neurons across the different cortical layers, microvessels and the choroid plexus reported here is generally consistent with previously published studies of human fetuses (Roberts *et al.* 2008; Wirth *et al.* 2009) and supports its role in TH uptake into the brain parenchyma from the blood and cerebrospinal fluid, as well as into neurons, from early fetal development.

Neurogenesis takes place in the ventricular and subventricular zones with much completed by 28 weeks gestation (Bystron *et al.* 2008). MCT8 staining in these neuroprecursor-rich areas at 19-26 weeks suggests its involvement in regulating neurogenesis. Indeed, we have previously demonstrated that MCT8 represses the proliferation of the human neuronal precursor cell, NT2, in a T_3-independent manner (James *et al.* 2009), however, MCT8 had no effect on NT2 neurodifferentiation *in vitro* (Chan *et al.* 2011). Post-mitotic neurons migrate away from the proliferative zones and by 24-28 weeks gestation most have

settled to form the cortical plate, an area comprising predominantly of neuronal cells (Bystron *et al.* 2008).

During normal human fetal cortical development over 70% of neurons undergo programmed cell death after 32 weeks of gestation (Rabinowicz *et al.* 1996). Magnetic resonance imaging (MRI) assessments of intrauterine growth-restricted premature infants at 33-34 weeks have shown reduced cerebral cortical gray matter volume (Tolsa *et al.* 2004), which could be due to reduced cell numbers in the cortical plate (Samuelsen *et al.* 2003). Similar to our IUGR cohort of 24-28 weeks, that study (Samuelsen *et al.* 2003), however, found no significant differences in cortical cell numbers compared with AGA before 27 weeks.

MCT8 promotes cell death in non-proliferative cytotrophoblast cells from human placenta independently of T_3 (Vasilopoulou *et al.* 2013). It remains speculative whether MCT8 could also have a similar effect on neuronal apoptosis. If so, down-regulation of MCT8 expression in IUGR neurons could be a protective mechanism to limit neuronal apoptosis at the expense of TH transport, of which the latter could be partially compensated for by other TH transporters expressed by neurons, as we and others of previously described in the human fetal cerebral cortex (Chan *et al.* 2011; Wirth *et al.* 2009).

Whether the reduction in cortical cell number in the third trimester is due to reduced neurogenesis, reduced neuronal migration or increased cell death in IUGR is not known. In rats, abnormal neuronal migration in the fetal CNS has been reported with both IUGR (Sasaki *et al.* 2000) and TH deficiency (Auso *et al.* 2004). Maternal TH deficiency in rats have also led to impaired neurogenesis and diminished neocortical neuronal numbers (Mohan *et al.* 2012). The extent to which these altered cellular processes in IUGR, as well as possibly altered synaptogenesis and dendritic branching, are mediated by diminished TH action secondary to reductions in circulating TH concentrations, MCT8 transport and TR expression remains the subject of investigation. Other factors such as cerebral hypoxia and prematurity, are also likely to contribute to this neuropathology. Whatever the etiologies, alterations in brain neural networks

assessed by MRI in IUGR infants have been associated with later neurodevelopmental outcomes (Batalle *et al.* 2012).

Current understanding of the physiological regulation of MCT8 expression is poor. TH status has influenced MCT8 expression in some tissues (Capelo *et al.* 2009) but not others (Mebis *et al.* 2009). In IUGR, MCT8 expression in the human placenta is upregulated (Vasilopoulou *et al.* 2010) in contrast to the fetal cerebral cortex. These tissue specific effects argue against a general alteration in MCT8 activity being part of the etiology of IUGR but rather suggest that altered cerebral MCT8 expression is a local adaptive response to the growth restricted state that is associated with chronic distress, which is supported by our finding that the greater the growth restriction the lower the MCT8 expression. This is in contrast to the AGA fetuses who presumably suffered from an acute event just prior to death. The positive correlation between MCT8 expression in the cortical plate and in microvessels suggests that there may be some common mechanisms regulating MCT8 expression in the CNS.

Future studies should investigate whether there are compensatory alterations in the expression of other TH transporters in neurons and microvessels. Studies could also extend to other regions of the CNS and at different gestational ages to obtain a more comprehensive picture of the effects of IUGR on TH transport and how this could correlate with observed neurological impairments in IUGR survivors.

In conclusion, our results showing perturbed patterns of cortical MCT8 expression support the hypothesis that a reduction in MCT8 expression in the IUGR fetal CNS could be a contributory factor implicated in the long term neurodevelopmental impairments associated with this condition.

Declaration of interest

All authors have nothing to declare.

Funding

This work was supported by the Health Foundation (Clinician Scientist Fellowship awarded to SYC; 6462/4335), Action Medical Research (SP4142 to JAF, SYC, MDK, CJM, AL), Medical Research Council UK (G0501548 to SYC, MDK, JAF, CJM) and the University of Birmingham.

Acknowledgements

We thank Aga Hussain for assistance with the immunohistochemistry.

Reference List

Auso E, Lavado-Autric R, Cuevas E, del Rey FE, Morreale De EG & Berbel P 2004 A moderate and transient deficiency of maternal thyroid function at the beginning of fetal neocorticogenesis alters neuronal migration. *Endocrinology* **145** 4037-4047.

Batalle D, Eixarch E, Figueras F, Munoz-Moreno E, Bargallo N, Illa M, Acosta-Rojas R, Amat-Roldan I & Gratacos E 2012 Altered small-world topology of structural brain networks in infants with intrauterine growth restriction and its association with later neurodevelopmental outcome. *Neuroimage.* **60** 1352-1366.

Bystron I, Blakemore C & Rakic P 2008 Development of the human cerebral cortex: Boulder Committee revisited. *Nat.Rev.Neurosci.* **9** 110-122.

Capelo LP, Beber EH, Fonseca TL & Gouveia CH 2009 The monocarboxylate transporter 8 and L-type amino acid transporters 1 and 2 are expressed in mouse skeletons and in osteoblastic MC3T3-E1 cells. *Thyroid* **19** 171-180.

Ceballos A, Belinchon MM, Sanchez-Mendoza E, Grijota-Martinez C, Dumitrescu AM, Refetoff S, Morte B & Bernal J 2009 Importance of monocarboxylate transporter 8 for the blood-brain barrier-dependent availability of 3,5,3'-triiodo-L-thyronine. *Endocrinology* **150** 2491-2496.

Chan S, Kachilele S, McCabe C, Tannahill L, Boelaert K, Gittoes N, Visser T, Franklyn J & Kilby M 2002 Early expression of thyroid hormone deiodinases and receptors in human fetal cerebral cortex. *Brain Res.Dev.Brain Res.* **138** 109-116.

Chan SY, Andrews MH, Lingas R, McCabe CJ, Franklyn JA, Kilby MD & Matthews SG 2005 Maternal nutrient deprivation induces sex-specific changes in thyroid hormone receptor and deiodinase expression in the fetal guinea pig brain. *Journal of Physiology-London* **566** 467-480.

Chan SY, Martin-Santos A, Loubiere LS, Gonzalez AM, Stieger B, Logan A, McCabe CJ, Franklyn JA & Kilby MD 2011 The expression of thyroid hormone transporters in the human fetal cerebral cortex during early development and in N-Tera-2 neurodifferentiation. *J.Physiol* **589** 2827-2845.

Cox P & Marton T 2009 Pathological assessment of intrauterine growth restriction. *Best.Pract.Res.Clin.Obstet.Gynaecol.* **23** 751-764.

Dowdeswell HJ, Slater AM, Broomhall J & Tripp J 1995 Visual deficits in children born at less than 32 weeks' gestation with and without major ocular pathology and cerebral damage. *Br.J.Ophthalmol.* **79** 447-452.

Dumitrescu AM, Liao XH, Best TB, Brockmann K & Refetoff S 2004 A novel syndrome combining thyroid and neurological abnormalities is associated with mutations in a monocarboxylate transporter gene. *American Journal of Human Genetics* **74** 168-175.

Friesema EC, Ganguly S, Abdalla A, Manning Fox JE, Halestrap AP & Visser TJ 2003 Identification of monocarboxylate transporter 8 as a specific thyroid hormone transporter. *J.Biol.Chem.* **278** 40128-40135.

Friesema ECH, Grueters A, Biebermann H, Krude H, von Moers A, Reeser M, Barrett TG, Mancilla EE, Svensson J, Kester MHA, Kuiper GGJM, Balkassmi S, Uitterlinden AG, Koehrle J,

Rodien P, Halestrap AP & Visser T 2004 Association between mutations in a thyroid hormone transporter and severe X-linked psychomotor retardation. *Lancet* **364** 1435-1437.

Garcia-Silva S, Perez-Juste G & Aranda A 2002 Cell cycle control by the thyroid hormone in neuroblastoma cells. *Toxicology* **181-182** 179-182.

Gardosi J, Chang A, Kalyan B, Sahota D & Symonds EM 1992 Customized Antenatal Growth Charts. *Lancet* **339** 283-287.

Gardosi J, Kady SM, McGeown P, Francis A & Tonks A 2005 Classification of stillbirth by relevant condition at death (ReCoDe): population based cohort study. *BMJ* **331** 1113-1117.

Gilbert ME & Paczkowski C 2003 Propylthiouracil (PTU)-induced hypothyroidism in the developing rat impairs synaptic transmission and plasticity in the dentate gyrus of the adult hippocampus. *Developmental Brain Research* **145** 19-29.

Heuer H & Mason CA 2003 Thyroid hormone induces cerebellar Purkinje cell dendritic development via the thyroid hormone receptor alpha1. *J Neurosci.* **23** 10604-10612.

James SR, Franklyn JA, Reaves BJ, Smith VE, Chan SY, Barrett TG, Kilby MD & McCabe CJ 2009 Monocarboxylate transporter 8 in neuronal cell growth. *Endocrinology* **150** 1961-1969.

Jones SA, Jolson DM, Cuta KK, Mariash CN & Anderson GW 2003 Triiodothyronine is a survival factor for developing oligodendrocytes. *Mol.Cell Endocrinol* **199** 49-60.

Kady M & Gardosi J 2004 Perinatal mortality and fetal growth restriction. *Best.Pract.Res.Clin.Obstet.Gynaecol.* **18** 397-410.

Kilby MD, Gittoes N, McCabe C, Verhaeg J & Franklyn JA 2000 Expression of thyroid receptor isoforms in the human fetal central nervous system and the effects of intrauterine growth restriction. *Clin.Endocrinol.(Oxf)* **53** 469-477.

Kilby MD, Verhaeg J, Gittoes N, Somerset DA, Clark PM & Franklyn JA 1998 Circulating thyroid hormone concentrations and placental thyroid hormone receptor expression in normal human pregnancy and pregnancy complicated by intrauterine growth restriction (IUGR). *J.Clin.Endocrinol.Metab* **83** 2964-2971.

Kok JH, den Ouden AL, Verloove-Vanhorick SP & Brand R 1998 Outcome of very preterm small for gestational age infants: the first nine years of life. *Br.J.Obstet.Gynaecol.* **105** 162-168.

Lavado-Autric R, Auso E, Garcia-Velasco JV, Arufe MD, del Rey FE, Berbel P & de Escobar GM 2003 Early maternal hypothyroxinemia alters histogenesis and cerebral cortex cytoarchitecture of the progeny. *Journal of Clinical Investigation* **111** 1073-1082.

Leitner Y, Fattal-Valevski A, Geva R, Eshel R, Toledano-Alhadef H, Rotstein M, Bassan H, Radianu B, Bitchonsky O, Jaffa AJ & Harel S 2007 Neurodevelopmental outcome of children with intrauterine growth retardation: a longitudinal, 10-year prospective study. *J.Child Neurol.* **22** 580-587.

Mebis L, Debaveye Y, Ellger B, Derde S, Ververs EJ, Langouche L, Darras VM, Fliers E, Visser TJ & Van den BG 2009 Changes in the central component of the hypothalamus-pituitary-thyroid axis in a rabbit model of prolonged critical illness. *Crit Care* **13** R147.

Mohan V, Sinha RA, Pathak A, Rastogi L, Kumar P, Pal A & Godbole MM 2012 Maternal thyroid hormone deficiency affects the fetal neocorticogenesis by reducing the proliferating pool, rate of neurogenesis and indirect neurogenesis. *Exp.Neurol.* **237** 477-488.

National Institute of Health. ***Quantifying Stained Liver Tissue***. 2012. http://rsbweb.nih.gov/ij/docs/examples/stained-sections/index.html

Rabinowicz T, de Court, Petetot JM, Xi G & de los RE 1996 Human cortex development: estimates of neuronal numbers indicate major loss late during gestation. *J.Neuropathol.Exp.Neurol.* **55** 320-328.

Roberts LM, Woodford K, Zhou M, Black DS, Haggerty JE, Tate EH, Grindstaff KK, Mengesha W, Raman C & Zerangue N 2008 Expression of the thyroid hormone transporters monocarboxylate transporter-8 (SLC16A2) and organic ion transporter-14 (SLCO1C1) at the blood-brain barrier. *Endocrinology* **149** 6251-6261.

Samuelsen GB, Larsen KB, Bogdanovic N, Laursen H, Graem N, Larsen JF & Pakkenberg B 2003 The changing number of cells in the human fetal forebrain and its subdivisions: a stereological analysis. *Cereb.Cortex* **13** 115-122.

Sasaki J, Fukami E, Mimura S, Hayakawa M, Kitoh J & Watanabe K 2000 Abnormal cerebral neuronal migration in a rat model of intrauterine growth retardation induced by synthetic thromboxane A(2). *Early Hum.Dev.* **58** 91-99.

Schwartz CE, May MM, Carpenter NJ, Rogers RC, Martin J, Bialer MG, Ward J, Sanabria J, Marsa S, Lewis JA, Echeverri R, Lubs HA, Voeller K, Simensen RJ & Stevenson RE 2005

Allan-Herndon-Dudley syndrome and the monocarboxylate transporter 8 (MCT8) gene. *American Journal of Human Genetics* **77** 41-53.

Tolsa CB, Zimine S, Warfield SK, Freschi M, Sancho RA, Lazeyras F, Hanquinet S, Pfizenmaier M & Huppi PS 2004 Early alteration of structural and functional brain development in premature infants born with intrauterine growth restriction. *Pediatr.Res.* **56** 132-138.

Trajkovic M, Visser TJ, Mittag J, Horn S, Lukas J, Darras VM, Raivich G, Bauer K & Heuer H 2007 Abnormal thyroid hormone metabolism in mice lacking the monocarboxylate transporter 8. *Journal of Clinical Investigation* **117** 627-635.

Vasilopoulou E, Loubiere LS, Heuer H, Trajkovic-Arsic M, Darras VM, Visser TJ, Lash GE, Whitley GS, McCabe CJ, Franklyn JA, Kilby MD & Chan SY 2013 Monocarboxylate transporter 8 modulates the viability and invasive capacity of human placental cells and fetoplacental growth in mice. *PLoS One* **8** e65402. doi: 10.1371/journal.pone.0065402.

Vasilopoulou E, Loubiere LS, Martin-Santos A, McCabe CJ, Franklyn JA, Kilby MD & Chan SY 2010 Differential Triiodothyronine Responsiveness and Transport by Human Cytotrophoblasts from Normal and Growth-Restricted Pregnancies. *J Clin.Endocrinol Metab*. **95** 4762-4770.

Wirth EK, Roth S, Blechschmidt C, Holter SM, Becker L, Racz I, Zimmer A, Klopstock T, Gailus-Durner V, Fuchs H, Wurst W, Naumann T, Brauer A, de Angelis MH, Kohrle J, Gruters A & Schweizer U 2009 Neuronal 3',3,5-triiodothyronine (T3) uptake and behavioral phenotype of mice deficient in Mct8, the neuronal T3 transporter mutated in Allan-Herndon-Dudley syndrome. *J Neurosci.* **29** 9439-9449.

Zoeller RT & Rovet J 2004 Timing of thyroid hormone action in the developing brain: clinical observations and experimental findings. *J.Neuroendocrinol.* **16** 809-818.

FIGURE LEGENDS

Figure 1: MCT8 immunohistochemistry of cerebral cortex sections obtained from structurally normal fetuses with unexplained intrauterine death. Corresponding negative controls (antibody-absorption by the blocking peptide) of adjacent sections are shown in panels inserted into the bottom right corner for A-C. At 19 weeks, MCT8 was located in the cortical plate within the parietal cortex (PC) with less staining in the marginal zone (MZ) (A), in the hippocampus (B) and the choroid plexus (CP) (C). MCT8 immunostaining was also seen in the ependymal cells lining the ventricle (V) and in numerous cells within the ventricular (VZ) and subventricular zone (SVZ) at 19 weeks (D), 26 weeks (E) and 37 weeks (F). MCT8 immunostaining in the wall of a microvessel in the subplate at 19 weeks (G), in neurons in the intermediate zone at 19 weeks (H) and 37 weeks (I; arrow points to a neuron). An adjacent section stained with GFAP is shown in a panel inserted into the bottom right corner for (H) showing differences in the morphology of immunostained cells. At 19 weeks, CD68 immunostaining for microglia (J) and GFAP immunostaining for glia (K) in the ventricular and subventricular zones showing a different pattern of staining to MCT8. There is also a lack of GFAP staining in the cortical plate and marginal zone of the parietal cortex at 19 weeks (L). Magnification bar = 50μm.

Figure 2: Quantification of MCT8 immunostaining in the occipital cerebral cortex of intrauterine growth restricted (IUGR) fetuses (n=7; black bars) compared with appropriately grown for gestational age (AGA) fetuses (n=5; white bars). The percentage area of cortical plate and the proportion of microvessels in the subplate immunostained for MCT8 are expressed relative to the mean of the AGA group, which has been given an arbitrary value of 1. Columns and error bars represent the mean and standard error of the mean. Statistically significant difference *$p<0.05$

Figure 3: Representative sections showing MCT8 immunostaining of the cortical plate of an intrauterine growth restricted (IUGR) fetus (A) and an appropriately grown for gestational age (AGA) fetus (B) within the occipital cerebral cortex. Corresponding negative controls (no primary antibody) of adjacent

sections are shown in a panel insert in the bottom right corner. An example of a positively MCT8 immunostained microvessel in the subplate (C) compared to a negative one (shown in a panel insert in the bottom right corner) from the same section immunostained for MCT8.

Figure 4: (A) The correlation between the relative cortical plate area immunostained with MCT8 and the relative proportion of microvessels immunostained with MCT8 in IUGR (black dots) and AGA (white squares) fetuses. A significant positive correlation is seen when all samples are considered together ( ) and wh~~en~~ ~~I~~UGR samples are considered on their own ( ) but ~~there~~ is no significant correlation amongst AGA samples on their own ( ). ~~(B)~~ ~~Th~~ere is a negative correlation between the relative cortical plate area immunostained with MCT8 and the brain to liver weight ratios when all samples are considered together. Statistically significant differences are **p<0.01, *p<0.05

Table legend:

Table 1: Characteristics of human stillbirth cases. ReCoDe is a classification system for stillbirths by relevant condition at death.(Gardosi *et al.* 2005) A7: Intrapartum asphyxia; A8: fetal growth restriction; A9: other fetal factor (in AGA3 it was pulmonary hypoplasia); B4: other umbilical cord (in IUGR7 it was umbilical vein thrombosis); C1: abruption; C4: placental infarction; C5: placental insufficiency; D2: oligohydramnios.

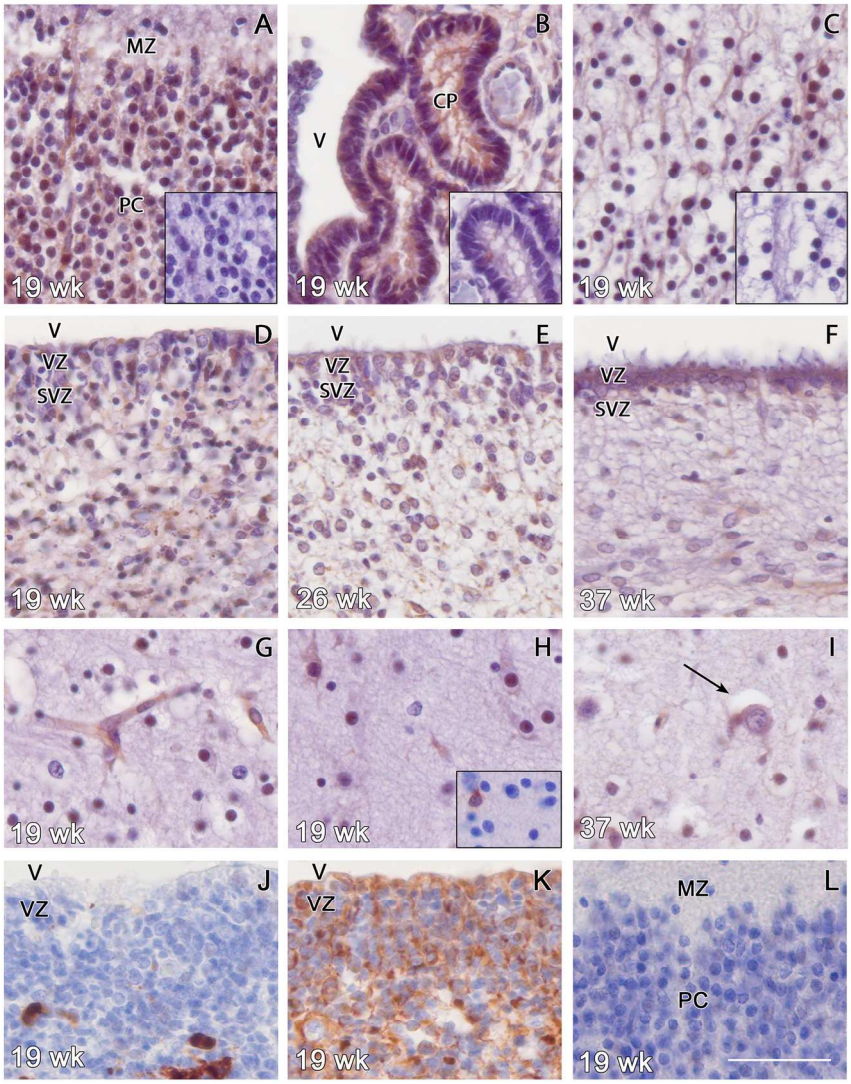

Figure 1: MCT8 immunohistochemistry of cerebral cortex sections obtained from structurally normal fetuses with unexplained intrauterine death. Corresponding negative controls (antibody-absorption by the blocking peptide) of adjacent sections are shown in panels inserted into the bottom right corner for A-C. At 19 weeks, MCT8 was located in the cortical plate within the parietal cortex (PC) with less staining in the marginal zone (MZ) (A), in the hippocampus (B) and the choroid plexus (CP) (C). MCT8 immunostaining was also seen in the ependymal cells lining the ventricle (V) and in numerous cells within the ventricular (VZ) and subventricular zone (SVZ) at 19 weeks (D), 26 weeks (E) and 37 weeks (F). MCT8 immunostaining in the wall of a microvessel in the subplate at 19 weeks (G), in neurons in the intermediate zone at 19 weeks (H) and 37 weeks (I; arrow points to a neuron). An adjacent section stained with GFAP is shown in a panel inserted into the bottom right corner for (H) showing differences in the morphology of immunostained cells. At 19 weeks, CD68 immunostaining for microglia (J) and GFAP immunostaining for glia (K) in the ventricular and subventricular zones showing a different pattern of staining to MCT8. There is also a lack of GFAP staining in the cortical plate and marginal zone of the parietal cortex at 19 weeks (L). Magnification bar =

50μm.
152x209mm (300 x 300 DPI)

Figure 2

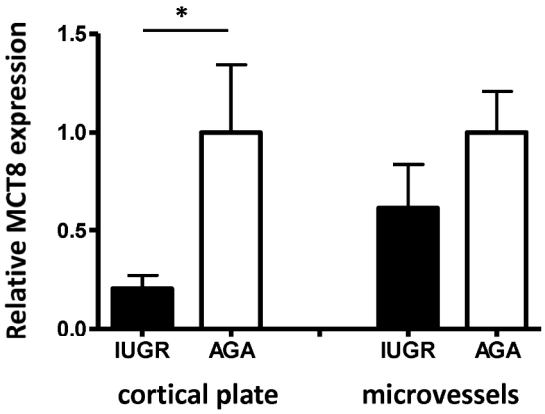

190x254mm (300 x 300 DPI)

Figure 3

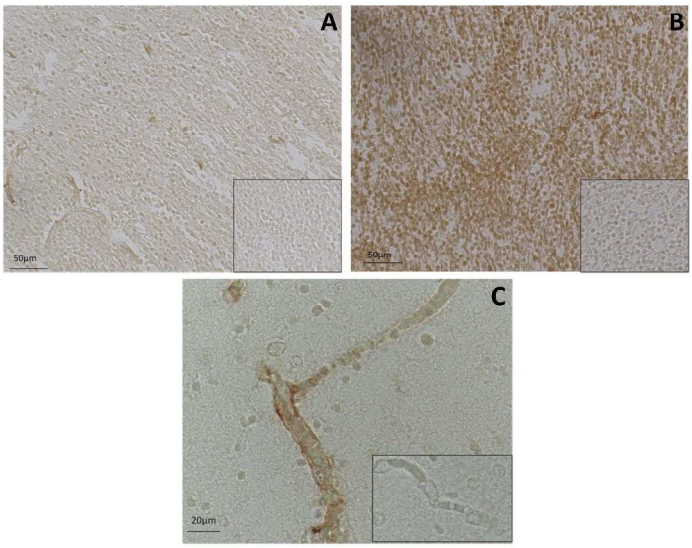

Figure 3: Representative sections showing MCT8 immunostaining of the cortical plate of an intrauterine growth restricted (IUGR) fetus (A) and an appropriately grown for gestational age (AGA) fetus (B) within the occipital cerebral cortex. Corresponding negative controls (no primary antibody) of adjacent sections are shown in a panel insert in the bottom right corner. An example of a positively MCT8 immunostained microvessel in the subplate (C) compared to a negative one (shown in a panel insert in the bottom right corner) from the same section immunostained for MCT8.
210x297mm (300 x 300 DPI)

Figure 4

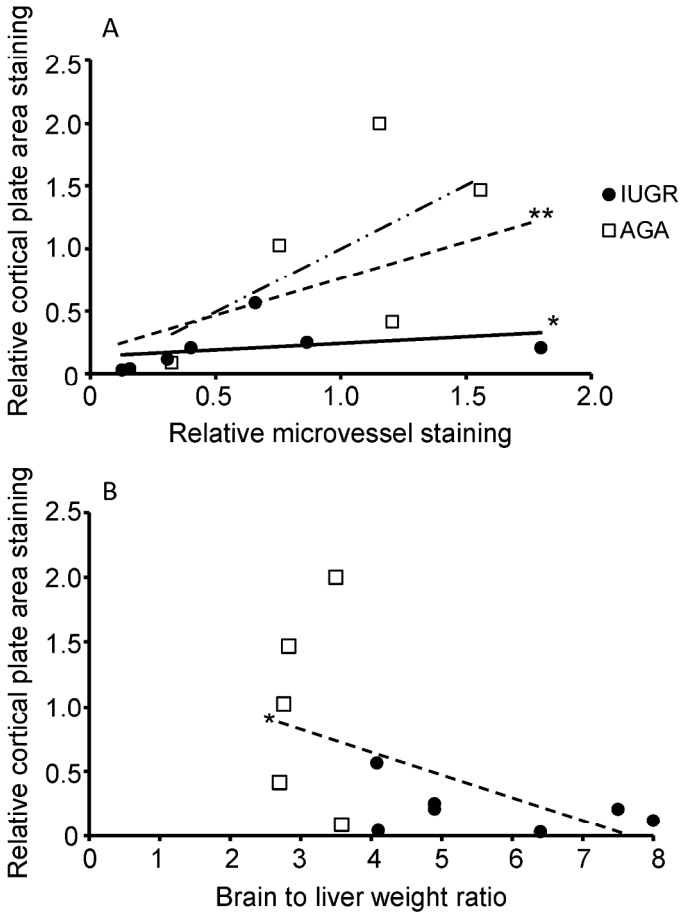

190x254mm (300 x 300 DPI)

Case	Gestation (weeks+ days)	Sex	Fetal weight (g) [Customized percentile (%)]	Brain weight (g)	Brain weight relative to expected mean for gestation	Brain:liver weight ratio	Thymus weight (g)	Thymus weight relative to expected mean for gestation	Cause of death (ReCoDe)
INTRAUTERINE GROWTH RESTRICTION									
IUGR 1	24+0	F	376 [<1]	76	0.92	4.9	0.2	0.13	antepartum asphyxia (A8 – cause unknown)
IUGR 2	26+0	M	643 [<1]	134	1.28	8.0	0.4	0.2	antepartum asphyxia (A8, C4)
IUGR 3	26+1	F	606 [<1]	117	1.11	4.9	0.4	0.2	antepartum asphyxia (A8, C4)
IUGR 4	26+3	M	592 [<1]	106	1.01	7.5	0.4	0.2	antepartum asphyxia (A8, C5)
IUGR 5	27+1	F	709 [<1]	130	1.10	4.1	1.2	0.52	antepartum asphyxia (A8, C1, C4)
IUGR 6	27+6	F	746 [<1]	135	1.14	6.4	1.4	0.61	antepartum asphyxia (A8, C5)
IUGR 7	28+2	M	906 [<1]	136	1.03	4.1	0.8	0.31	antepartum asphyxia (A8, B4, C4)
Mean ± SEM	*26.6 ± 0.5 weeks*	*M:F 3:4*	*654 ± 61*	*119 ± 8*	*1.08 ± 0.04*	*5.7 ± 0.6*	*0.69 ± 0.17*	*0.31 ± 0.07*	
APPROPRIATELY GROWN FOR GESTATIONAL AGE									
AGA1	24+2	M	732 [75]	102	1.23	3.5	1.4	0.93	intrapartum asphyxia (A7, C1)
AGA2	25+0	F	688 [50]	105	1.12	2.7	2.5	1.39	antepartum asphyxia (C1)
AGA3	26+2	M	863 [10]	123	1.17	2.8	1.5	0.75	intrapartum asphyxia (A9, D2)
AGA4	26+6	F	938 [77]	131	1.25	2.8	2.5	1.25	intrapartum asphyxia (C1)
AGA5	28+1	M	1156 [34]	176	1.49	3.6	3.8	1.65	antepartum asphyxia (C1)
Mean ± SEM	*26.1 ± 0.7 weeks*	*M:F 3:2*	*875 ± 83*	*127 ± 13*	*1.25 ± 0.06*	*3.1 ± 0.2*	*2.34 ± 0.43*	*1.19 ± 0.16*	
P value (IUGR vs	*NS*	*NS*	*0.05*	*NS*	*0.049*	*0.006*	*0.003*	<0.001	

AGA)

Table 1